Proceedings Paper:
Ouyang, X., Long, H. orcid.org/0000-0003-1673-1193 and Crawforth, P. (2025) Simulation and analysis of low-frequency vibrations in rotational vibration-assisted incremental sheet forming. In: Journal of Physics: Conference Series. The 13th International Conference and Workshop on Numerical Simulation of 3D Sheet Metal Forming Processes, 07-11 Jul 2025, Munich, Germany. ISSN: 1742-6588. EISSN: 1742-6596.

https://doi.org/10.1088/1742-6596/3104/1/012080

Journal of Physics:
Conference Series

PAPER • **OPEN ACCESS**

Simulation and Analysis of Low-frequency Vibrations in Rotational Vibration-assisted Incremental Sheet Forming

To cite this article: Xuan Ouyang *et al* 2025 *J. Phys.: Conf. Ser.* **3104** 012080

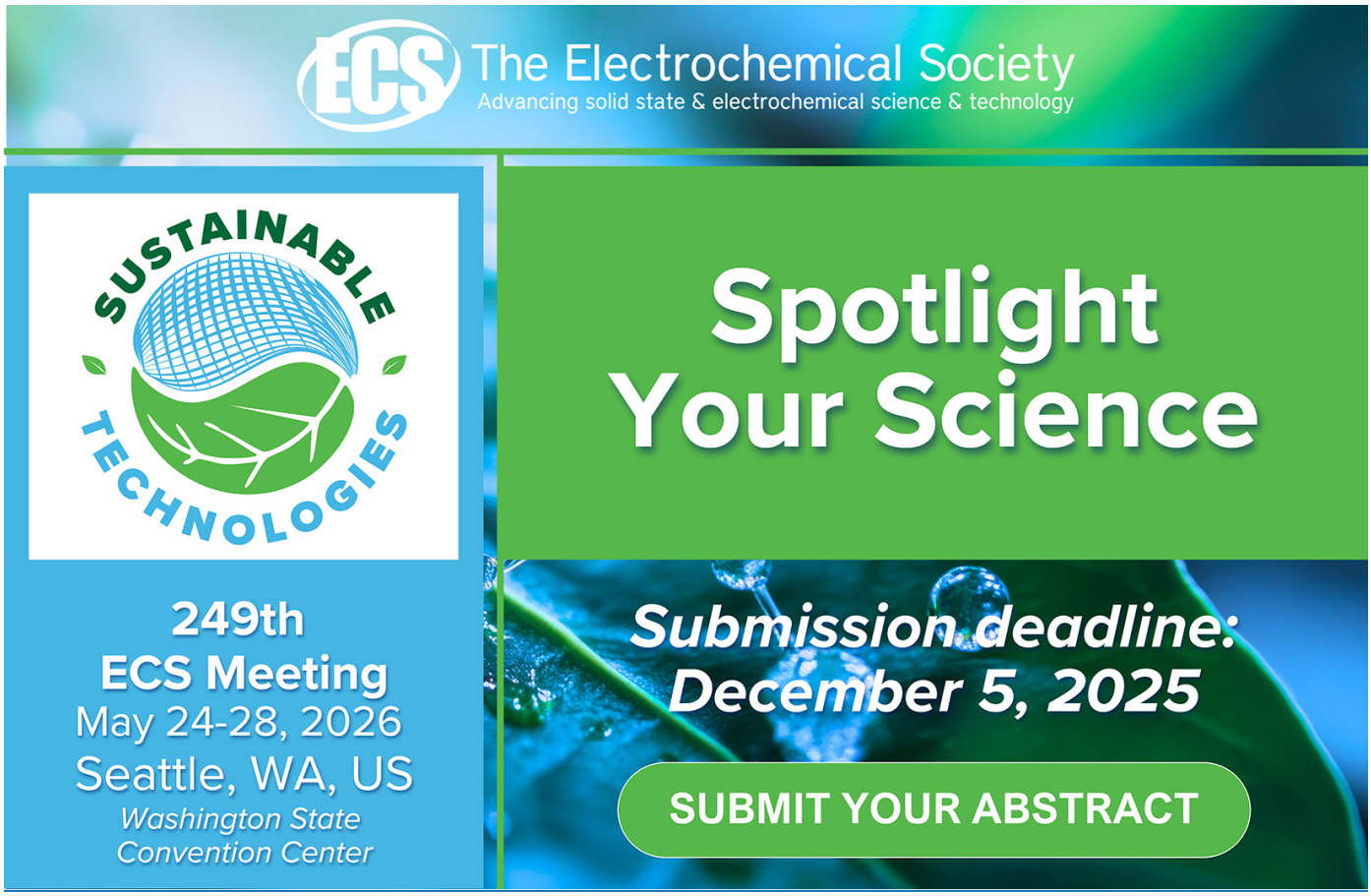

Journal of Physics: Conference Series **3104** (2025) 012080 doi:10.1088/1742-6596/3104/1/012080

Simulation and Analysis of Low-frequency Vibrations in Rotational Vibration-assisted Incremental Sheet Forming

Xuan Ouyang[1], Hui Long[1*] and Pete Crawforth[2]

[1] School of Mechanical, Aerospace and Civil Engineering, the University of Sheffield, Sheffield, S1 3JD, UK
[2] Advanced Manufacturing Research Centre, the University of Sheffield, Rotherham, S60 5TZ, UK

[*]E-mail: h.long@sheffield.ac.uk

Abstract. Incremental sheet forming (ISF) has demonstrated its potential of flexible manufacturing for low-volume or prototyping applications. Rotational vibration-assisted incremental sheet forming (RV-ISF) is a new process variant that advances the capability of the ISF technology for processing hard-to-form materials. New tools have been developed for RV-ISF, including a double offset tool and quad-grooved tool, to induce low-frequency vibrations into the deformed sheet in the range of 50-300 Hz, created by tool rotations. These imparted low-frequency vibrations result in vibration softening phenomena of the material which has been shown to lead to improvements in formability. However, the nature of the vibration generated during this new process and its impact on forming force reduction and softening effect have yet to be thoroughly examined. In this paper, a finite element model is developed to simulate the vibration of the sheet material induced by the RV-ISF tool, with the aim to predict the vibration frequency and amplitude during the process. The results show that the tool induced sheet vibration is localised at the tool-sheet contact which is validated by experimental measurement results. The frequency of the sheet vibration is dependent on the rotational speed and the number of grooves or offsets of the tool, while the vibration amplitude is associated with formed geometry and the tool design.

1. Introduction

Incremental Sheet Forming (ISF) has emerged as a highly flexible metal forming process. Compared to traditional sheet forming processes such as stamping, ISF offers significant advantages such as low cost, reduced lead time and high flexibility. These advantages make ISF particularly suitable for prototyping and low volume production [1]. As a result, ISF has been extensively studied over the past two decades, leading to the development of several process variants, including electric heating ISF [2], friction stir ISF [3], ultrasonic vibration assisted ISF [4] and hybrid ISF [5], which have been designed to address specific challenges such as formability, geometric accuracy and surface finish. While these variants have improved the conventional ISF process, they have also introduced new challenges such as increased process complexity, tool wear and surface defects. Recently a new variant, Rotational Vibration-assisted Incremental Sheet Forming (RV-ISF), has been developed [6]. This new variant offers distinct

advantages over other ISF variants by designing new rosette tools that can reduce forming forces, improve formability and achieve better surface quality at no additional requirement, retaining high flexibility and low cost of the ISF. In RV-ISF, the vibrations are generated by the rotational movement of tools, such as the double offset tool and quad-grooved tool, producing frequencies in the range of 50-300 Hz. The vibration-induced softening effect has been observed to improve the material formability, yet the underlying mechanisms governing this phenomenon remain insufficiently understood. Specifically, the nature of the induced vibrations, their localisation at the tool-sheet interface, and individual influences of vibration frequency and amplitude on forming force reduction require further investigation.

Previous study [6] has indicated that the vibration and frictional heating are generated during the RV-ISF process, both of which in combination contribute to material softening. While the thermal effects on material behaviour have been extensively investigated [7], the influence of vibrations, particularly at low frequencies (50-300 Hz in the RV-ISF conditions) on the material deformation behaviour, remains unclear. Although high-frequency vibration has been shown to be effective in reducing flow stress and surface friction due to the volume and surface effects [8], the role of low-frequency vibrations in the RV-ISF process has yet to be fully understood. Therefore, it is crucial to systematically evaluate the impact of vibrations on the forming process in RV-ISF to gain new insights into its material deformation under low-frequency vibration to support optimisation of process parameters of RV-ISF.

This study aims to bridge this gap by developing a finite element (FE) model to simulate the vibration behaviour of the sheet during RV-ISF. The model incorporates tool-induced vibrations and captures displacement variations at multiple locations when the sheet material is being deformed by the newly designed tool. The study analyses the distribution of vibration amplitudes of the sheet at various locations to understand how local stiffness and distance from the tool influence vibration behaviour. Additionally, an experimental validation is conducted to confirm the accuracy of the FE simulation results. The findings of this study will contribute to the optimization of RV-ISF process for improved manufacturability of hard-to-form materials.

2. Modelling and Experimental Methods

2.1 Finite Element Vibration Model

To predict the vibration characteristics (frequency and amplitude) of sheet induced by tool rotation in RV-ISF, a finite element model is developed using ABAQUS. This model simulates the localised vibrations of the sheet caused by tool rotation during the forming of a pyramid-shaped

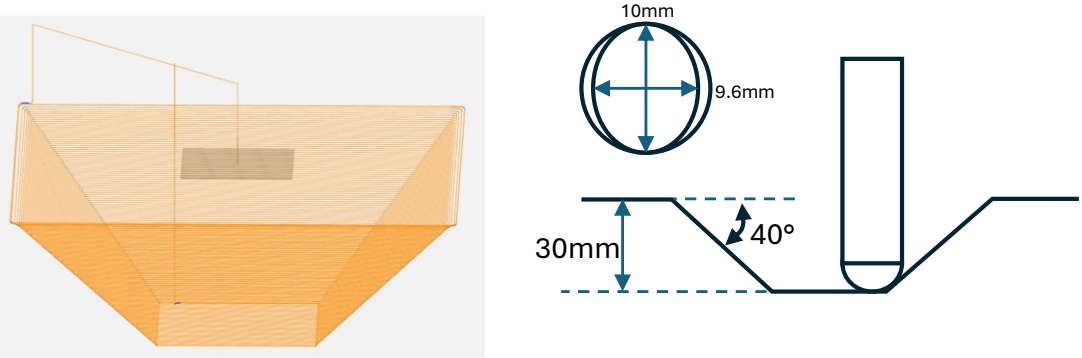

Figure 1. Tool path and formed pyramid geometry

geometry. The target geometry is a pyramid with a depth of 30 mm and a sidewall angle of 40°, as illustrated in Figure 1.

The material used in the simulation is AA6082-T6 with an initial thickness of 1 mm. The flow stress of the material, shown in Figure 2, is obtained from a uniaxial tensile test and implemented in the model. Since ISF simulation is computationally expensive, often requiring up to a week for a full process simulation, the inclusion of vibration effect further increases the computational load, the simulation does not start from deformation of a flat sheet. Instead, a pre-formed pyramid geometry with a depth of 20 mm and a 40° sidewall angle is generated using CAD software and then imported into ABAQUS as a 3D deformable part. Since the thickness of the sheet is significantly smaller than the other dimensions, shell elements are used to model the sheet. Compared to solid elements, shell elements can significantly reduce computation time while maintaining a reasonable simulation accuracy. Therefore, the sheet is meshed using 4-node, reduced-integration shell elements (S4R) with a mesh size of 0.5 mm to ensure an accurate representation of deformation and vibration behaviour. Five integration points are assigned through thickness direction to simulate the bending effect.

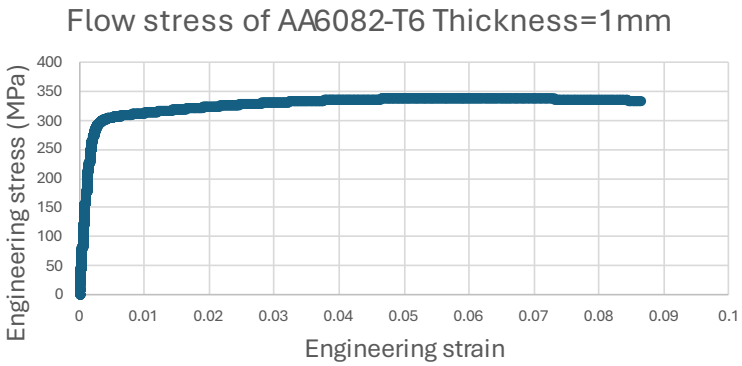

Figure 2. Flow stress of AA6082-T6

Since material thickness plays a critical role in vibration amplitude during forming, it is essential to replicate the thickness distribution of the pre-formed pyramid accurately. In ISF, as there is no material inflow, shape formation occurs purely through plastic deformation, leading to thickness reduction following the cosine law [9]. Given that the sidewall angle of the formed geometry is 40°, the resulting sheet thickness is set to 0.766 mm to reflect actual forming conditions. A double-offset tool (T2) is imported into ABAQUS as a rigid body and meshed with 8-node linear reduced-integration 3D solid elements (C3D8R). This tool has a diameter of 10 mm and two offsets of 0.2 mm on each side of the hemispherical tool head, as shown in Figure 3(a). Due to its double-offset design, the tool will impart the sheet twice per revolution.

To simulate the effect of clamping and boundary condition, the flat region on the boundary of the sheet is fully constrained while the central region remains free, allowing for deformation and vibration during the forming process. The interaction between the tool and the sheet is defined using a surface-to-surface contact with a friction coefficient of 0.05. The motion of the tool is controlled through a reference point located at the centre of the hemisphere of the tool, which determines both translational and rotational movements. Specifically, the tool can move freely along the X, Y, and Z directions, and rotate around the Z-axis. At the start of the simulation, the tool is positioned at one corner of the pyramid wall and subsequently rotates at a speed of

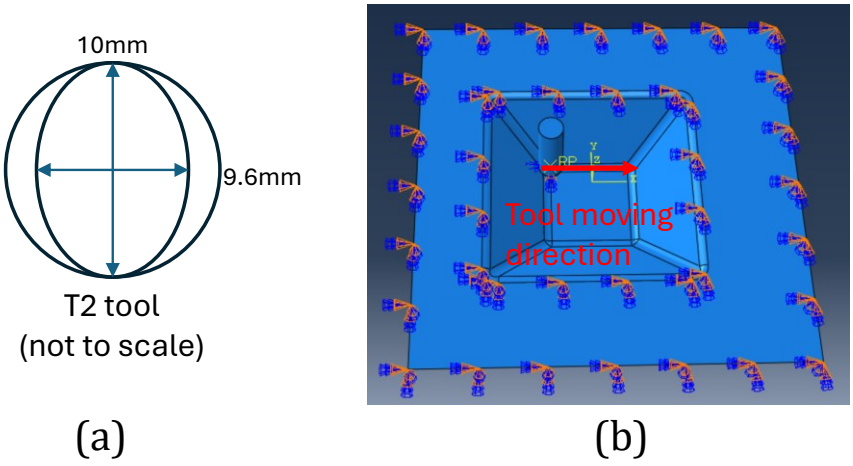

Figure 3. (a) Double-offset tool (T2); (b) Tool feed direction

3000 rpm while moving along the sidewall toward the adjacent corner, simulating a quarter-circle forming process, as shown in Figure 3(b).

The dynamic explicit solution method is used to solve the model of the forming process. Mass scaling technique with a target time increment of 1e-6 is used to improve computational efficiency while maintaining numerical accuracy. The time increment remains stable around 1e-6s throughout the simulation and the artificial energy is kept below 3% of the internal energy, which demonstrates the stability and reliability of the model.

2.2 Experiment Setup

To validate the accuracy of the FE simulation and analysis, the vibration of the sheet induced by tool rotation in the RV-ISF process is measured by using an eddy current sensor. This non-contact sensor captures the local displacement of the sheet, enabling further analysis of vibration frequency and amplitude.

To ensure consistency between the experiment and simulation, the pyramid-shaped geometry is first formed without measurement to assist the determination of the sensor location. Afterward, the eddy current sensor is positioned at a depth of 20 mm, maintaining a 1 mm distance from the sidewall, as illustrated in Figure 4. During the subsequent forming process, as

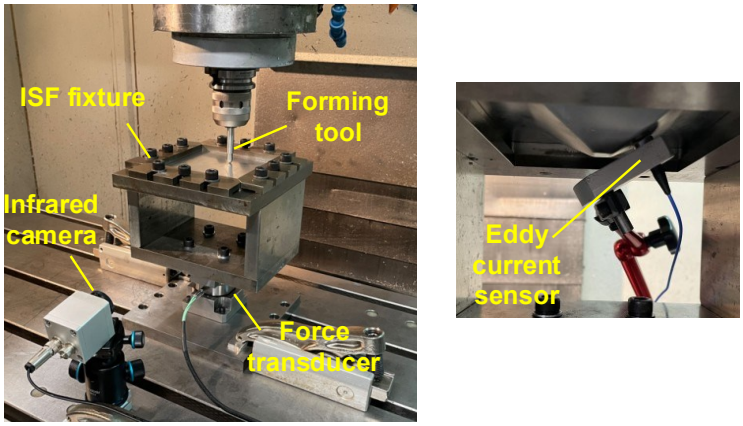

Figure 4. Setup of RV-ISF and the position of eddy current sensor

the tool moves deeper and passes through the region where the sensor is located, the vibration of the sheet induced by tool rotation is continuously recorded with high precision. This setup ensures that the collected vibration data accurately represent the dynamic response of the sheet under actual forming conditions.

2.3 Data Extraction and Processing

To evaluate the vibration characteristics induced by tool rotation in RV-ISF and compare them with experimental results, displacement data is extracted from the FE simulation. The nodal displacements of the sheet are recorded in the X, Y, and Z directions at multiple key locations to analyse vibration amplitude and frequency. The displacements in the Y and Z directions are combined to represent the out-of-plane displacement of the sheet, which is the thickness direction, while the X-direction displacement corresponds to the in-plane displacement.

Nodes are selected along two key directions in order to analyse the vibration characteristics. The first one is along the tool movement path, where points are chosen every 4 mm, with Node h1 at the starting position and Node h8 at the endpoint of the bottom of the formed section of the pyramid. This allows for the investigation of how tool movement influences sheet vibration. The second direction is along the sidewall at the centre of the formed section of the pyramid, where points are selected every 2 mm, with Node v1 closest to the tool and Node v12 farthest, enabling the analysis of vibration distribution along the sidewall height. The displacement of these nodes is recorded as history outputs, and their locations are illustrated in Figure 5.

After selecting an appropriate time window for analysis, the vibration spectrum at each node is extracted using centralization and Fast Fourier Transform (FFT). Centralization is performed to eliminate the zero-frequency component of the signal, while FFT converts the time-domain displacement data into the frequency domain, enabling the identification of dominant vibration modes. The vibration amplitude is determined by analysing the peak-to-peak displacement of selected nodes over time.

Similarly, for the measurement data from the ISF experiment, the time-displacement data obtained from the non-contact eddy current sensor is processed using the same method as that used to the FE simulation data to extract the actual vibration characteristics. To ensure accuracy, a sampling rate of 4000 Hz is used for both simulation and experiment, enabling precise capture of the dynamic response of the sheet.

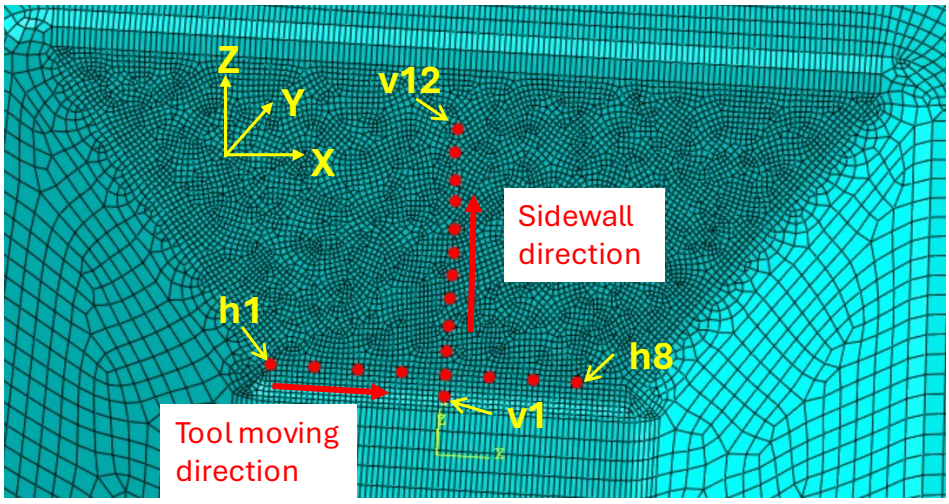

Figure 5. Positions of selected nodes for analysis

3. Results and Discussion

3.1 Node Displacement and Data Processing

The displacement data for a representative node h5 (5th point along the tool path direction) is presented in Figure 6(a). It is observed that the displacement and vibration along the X direction are minimal compared to those along the Y and Z directions and can therefore be considered negligible. This is because the tool moves along the X-axis, while the vibrations induced by tool rotation predominantly occur perpendicular to the tool feed plane. Consequently, the displacement components in the Y and Z directions are combined to represent the out-of-plane displacement, which is the primary focus when analysing the vibration behaviour of the sheet.

The displacement responses of node h5, both parallel and perpendicular to the tool feed plane, are illustrated in Figure 6(b). The result shows that the vibration amplitude initially increases and then decreases over time. The maximum vibration occurs when the tool is in close

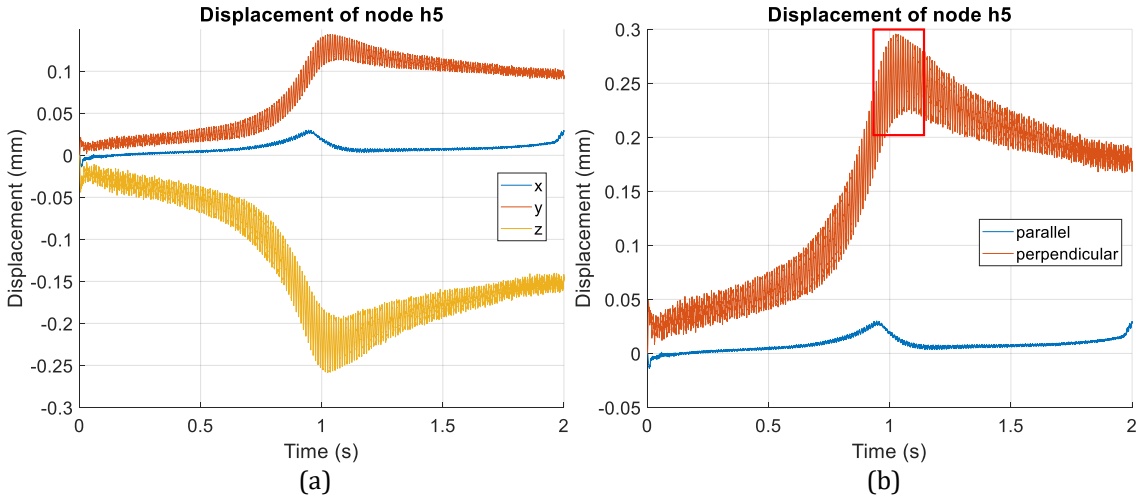

Figure 6. (a) Displacement of node h5 in x, y and z direction; (b) Displacement of node h5 parallel and perpendicular to the tool feed plane

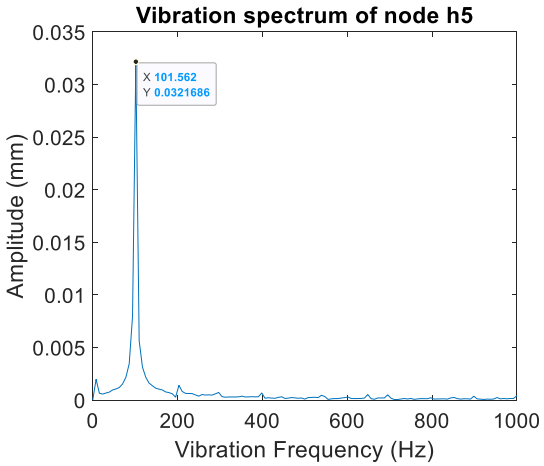

Figure 7. Vibration spectrum of node h5 after centralisation and Fast Fourier Transformation of displacement data

proximity to the node. Therefore, the displacement data corresponding to this peak vibration, highlighted in the red box, is selected for further analysis.

By performing centralization and Fast Fourier transformation, the resulting vibration spectrum for the selected node is shown in Figure 7. The vibration frequency is 101.562 Hz, and the corresponding vibration amplitude is 0.032 mm. The analysis reveals that the dominant vibration frequency closely matches the reference frequency (100Hz), which is theoretically determined based on the rotational speed and the number of offsets of the tool. The reference frequency is calculated using the equation:

$$f = \frac{S * N}{60}$$

where S is the rotational speed in revolutions per minute (rpm), and N is the number of offsets. This agreement between the measured and theoretical frequencies validates the accuracy of the vibration frequency analysis of the FE simulation data.

3.2 Vibration Response and Amplitude Distribution Along the Tool Path

Figure 8(a) presents the displacement responses of the selected nodes along the tool moving direction. The displacement of each node increases as the tool approaches, reaching its peak value when the tool is in close proximity. As the tool moves away, the displacement gradually decreases. A similar trend is observed in the vibration amplitude, which also reaches its maximum when the tool is nearby and gradually diminishes as the tool moves away. This indicates that the sheet vibration effect induced by tool rotation is highly localized during the forming process.

Figure 8(b) illustrates the maximum vibration amplitude of each node along the tool feed direction. The results show that the nodes at the two ends exhibit smaller amplitudes, while those in the middle region experience larger amplitudes. The node at the centre, node h5, has the largest amplitude, which is 0.032 mm. This pattern may be attributed to variations in structural stiffness within the pyramid-shaped geometry. Nodes located near the corners of the pyramid are regions likely having higher stiffness, which restricts their vibration. Conversely, nodes in the middle region, where the structure is relatively more flexible, exhibit greater vibration amplitudes. These findings suggest that the local stiffness of the formed geometry significantly influences the vibration response of the sheet, with less constrained regions experiencing higher vibration amplitudes.

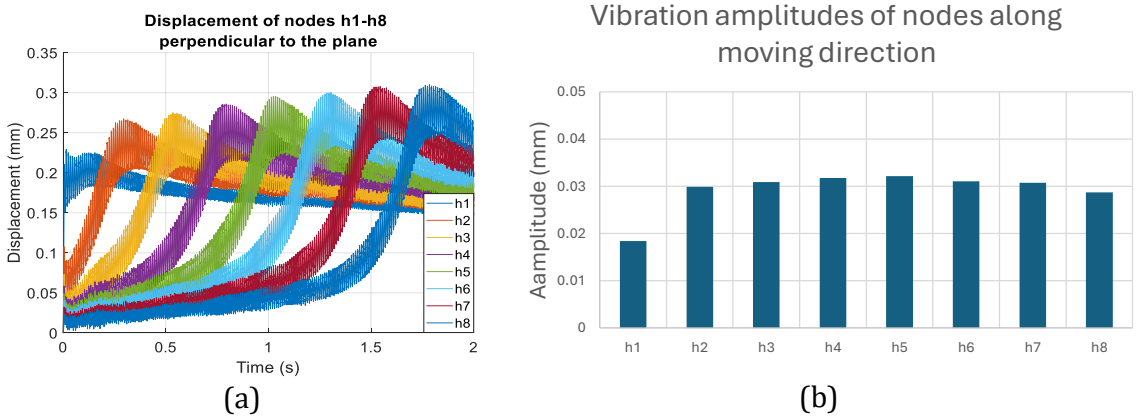

Figure 8. (a) Displacement response of the selected nodes along the tool moving direction; (b) Maximum vibration amplitudes of nodes along the moving direction

3.3 Vibration Response and Amplitude Distribution Along the Sidewall Direction

Figure 9(a) presents the displacement response of the selected nodes along sidewall direction. As observed, the displacement of each node increases as the tool approaches, reaching a peak less than one second, before gradually decreasing as the tool moves away. This confirms that the rotational movement of the tool induces localized vibrations, which propagate through the sheet and reduce with increasing distance from the tool position. Furthermore, the displacement curves exhibit a clear correlation between node position and vibration amplitude, with nodes closer to the tool experiencing more concentrated vibrations with larger amplitudes.

To further analyse this trend, the maximum vibration amplitudes of the selected nodes are extracted and plotted in Figure 9(b). In general, the vibration amplitude first increases and then decreases as the distance from the tool-sheet contact point increases, reaching the peak of 0.048 mm at node v4. This phenomenon can be attributed to the increased stiffness of the bottom node (Node v1), which is located near the bottom of the formed pyramid, thereby restricting its vibration. As the distance from the tool increases, the nodes have greater freedom of movement, allowing for larger vibration amplitudes. As the distance from the tool continues to increase, the nodes become less constrained, but they also experience weaker excitation directly from the tool rotation, leading to a gradual reduction in maximum vibration amplitude.

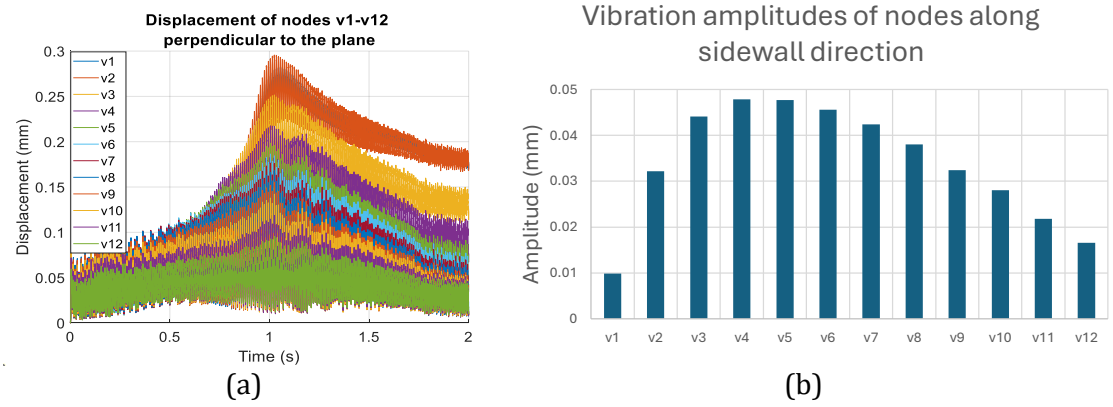

Figure 9. (a) Displacement response of the selected nodes along the sidewall direction; (b) Maximum vibration amplitudes of nodes along sidewall direction

3.4 Validation of FE Simulation Results by Experiment Measurement

To assess the accuracy of the FE vibration model in predicting sheet vibration characteristics, the vibration spectrum obtained from both the simulation and experiment are compared, as presented in Figure 10. The results demonstrate a good fit, with both exhibiting a dominant peak around 100 Hz, indicating the reliability of the FE simulation in capturing the primary vibration characteristics. The simulation results also show additional peaks near 300 Hz and 550 Hz, which are absent in the experimental data. This difference may be attributed to the simplified assumptions in the FE simulation model, particularly the use of homogeneous material properties, which could introduce additional resonance frequencies.

The comparison of vibration frequency and maximum amplitude are presented in Table 1. The results show that both the simulated and experimental vibration frequencies are very close to the reference frequency (100 Hz). The simulated frequency (101.562 Hz) exhibits a minor deviation of 1.6%, while the experimental frequency (99.6 Hz) deviates by only 0.4%. These small

differences suggest that the vibration characteristics are predominantly governed by the rotational speed and design of the tool, and that the FE vibration model provides a highly accurate representation of the frequency response.

Similarly, the predicted vibration amplitude (0.048 mm) by the FE vibration model is slightly higher than the experimental measurement (0.044 mm), with a relative error of approximately 9%. One possible reason for this difference is that the simulation does not fully account for the stress-strain relation of the sheet during the forming process. In the actual experiment, the material undergoes plastic deformation and work hardening, which could influence the stiffness of the sheet and vibration response. However, in the FE simulation, a predefined geometry is used, and the exact strain-hardening of the material is not captured. This discrepancy may lead to an overestimation of the vibration amplitude by the FE model. Future work needs to focus on incorporating strain evolution into the simulation model to further refine the accuracy of vibration predictions and enhance its applicability in process optimization. On the other hand, the current model uses a predefined flow stress curve derived from uniaxial tensile tests to represent plastic deformation, which may contribute to the observed amplitude discrepancies. Incorporating strain-hardening and evolving material behaviour will be considered in future studies to enhance prediction accuracy.

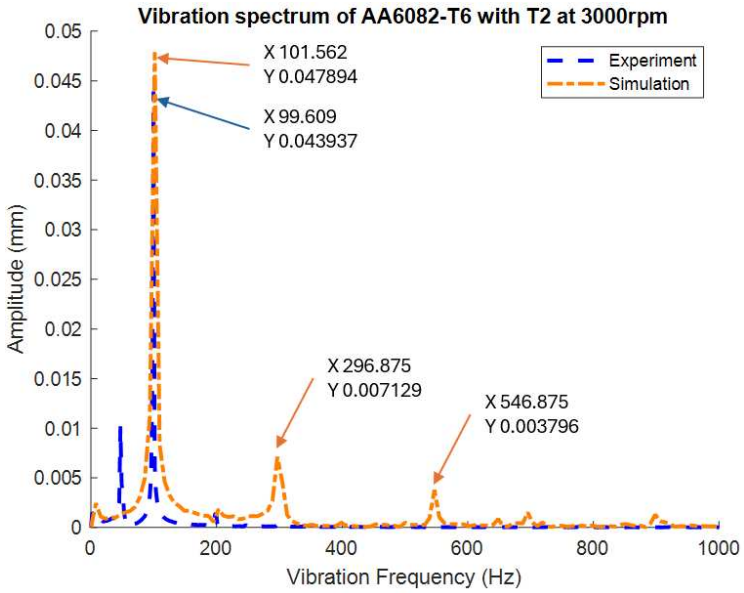

Figure 10. (a) Displacement response of the selected nodes along the sidewall direction; (b) Maximum vibration amplitudes of nodes along sidewall direction

Table 1. Comparison of vibration characteristics of simulation and experiment

	Vibration frequency (Hz)	Vibration amplitude (mm)
Simulation	101.562	0.048
Experiment	99.6	0.044
Reference	100	

4. Conclusions

This study investigates the vibration characteristics of the sheet induced by tool rotation in the new RV-ISF process through both FE simulation and experimental measurement. A FE vibration model is developed in ABAQUS to predict the vibration response, and experimental validation is conducted to measure the local displacement of the sheet. The following conclusions are drawn from the study:

- The vibration frequency obtained from both the simulation and experiment closely matches the reference frequency, confirming that the primary vibration mode is governed by the rotational speed and design of the tool.
- The vibration amplitude obtained from the simulation is also in good agreement with the experimental measurement, indicating that the simulation model can effectively capture the vibration characteristics in RV-ISF.
- The variation of the vibration amplitude in different directions reveals that tool-induced vibration of the deforming sheet in RV-ISF is localised, with its magnitude being influenced by local stiffness of the sheet and the tool design.

This study provides a quantitative understanding of the localised tool-induced vibration behaviour in RV-ISF, demonstrating that FE vibration simulation can serve as an effective approach for supporting the tool design and process optimisation.

5. Acknowledgements

The authors acknowledge the financial support received from the UK Engineering and Physical Sciences Research Council (EPSRC) through project grants EP/W010089/1 and EP/T005254/1. The first author would like to acknowledge the support of the Postgraduate Research Scholarship received from the University of Sheffield.

References

[1] J. R. Duflou *et al.*, 'Single point incremental forming: state-of-the-art and prospects', *Int. J. Mater. Form.*, vol. 11, no. 6, pp. 743–773, Nov. 2018, doi: 10.1007/s12289-017-1387-y.
[2] G. Fan, L. Gao, G. Hussain, and Z. Wu, 'Electric hot incremental forming: A novel technique', *Int. J. Mach. Tools Manuf.*, vol. 48, no. 15, pp. 1688–1692, Dec. 2008, doi: 10.1016/j.ijmachtools.2008.07.010.
[3] Z. Wang, S. Cai, and J. Chen, 'Experimental investigations on friction stir assisted single point incremental forming of low-ductility aluminum alloy sheet for higher formability with reasonable surface quality', *J. Mater. Process. Technol.*, vol. 277, p. 116488, Mar. 2020, doi: 10.1016/j.jmatprotec.2019.116488.
[4] M. Vahdati, R. Mahdavinejad, and S. Amini, 'Investigation of the ultrasonic vibration effect in incremental sheet metal forming process', *Proc. Inst. Mech. Eng. Part B J. Eng. Manuf.*, vol. 231, no. 6, pp. 971–982, May 2017, doi: 10.1177/0954405415578579.
[5] B. Lu, H. Zhang, D. K. Xu, and J. Chen, 'A Hybrid Flexible Sheet Forming Approach towards Uniform Thickness Distribution', *Procedia CIRP*, vol. 18, pp. 244–249, 2014, doi: 10.1016/j.procir.2014.06.139.
[6] H. Long, W. X. Peng, Z. D. Chang, H. Zhu, Y. J. Jiang, and Z. H. Li, 'New rosette tools for developing rotational vibration-assisted incremental sheet forming', *J. Mater. Process. Technol.*, vol. 326, p. 118311, May 2024, doi: 10.1016/j.jmatprotec.2024.118311.
[7] X. Zhan, X. Liu, M. Yang, M. Li, X. Li, and J. Chen, 'Dynamic recrystallization and solute precipitation during friction stir assisted incremental forming of AA2024 sheet', *Mater. Charact.*, vol. 174, p. 111046, Apr. 2021, doi: 10.1016/j.matchar.2021.111046.
[8] G. Shao, H. Li, and M. Zhan, 'A Review on Ultrasonic-Assisted Forming: Mechanism, Model, and Process', *Chin. J. Mech. Eng.*, vol. 34, no. 1, p. 99, Dec. 2021, doi: 10.1186/s10033-021-00612-0.
[9] D. Young and J. Jeswiet, 'Wall thickness variations in single-point incremental forming', *Proc. Inst. Mech. Eng. Part B J. Eng. Manuf.*, vol. 218, no. 11, pp. 1453–1459, Nov. 2004, doi: 10.1243/0954405042418400.